Received: 23 October 2017 | Revised: 24 May 2018 | Accepted: 31 May 2018

DOI: 10.1002/we.2222

RESEARCH ARTICLE

WILEY

Multiline anchor force dynamics in floating offshore wind turbines

Casey M. Fontana[1] | Spencer T. Hallowell[1] | Sanjay R. Arwade[1] | Don J. DeGroot[1] | Melissa E. Landon[2] | Charles P. Aubeny[3] | Brian Diaz[3] | Andrew T. Myers[4] | Senol Ozmutlu[5]

[1]University of Massachusetts Amherst, Marston Hall, 130 Natural Resources Road, Amherst, Massachusetts 01003, USA

[2]University of Maine, 319B Boardman Hall, Long Road, Orono, Maine 04469, USA

[3]Texas A&M University, 199 Spence Street, College Station, Texas 77840, USA

[4]Northeastern University, 439 Snell Engineering Center, 360 Huntington Avenue, Boston, Massachusetts 02115, USA

[5]Vyrhof Anchors, Rhijnspoor 255, 2901 LB Capelle aan den IJssel, The Netherlands

Correspondence
Casey M. Fontana, Department of Civil Engineering, University of Massachusetts Amherst, Marston Hall 236, 130 Natural Resources Road, Amherst, Massachusetts 01003, USA.
Email: cfontana@umass.edu

Funding information
Division of Civil, Mechanical and Manufacturing Innovation, Grant/Award Numbers: 1462600, 1463273 and 1463431; Division of Graduate Education, Grant/Award Number: 1068864; Massachusetts Clean Energy Center

Abstract

Floating offshore wind energy has seen significant progress, evidenced by multiple demonstration projects and the first floating wind farm (Hywind Scotland). However, the high capital cost associated with floating wind development remains one of the primary hurdles in the industry's growth. In efforts to lower this cost, this paper investigates a novel shared anchor concept to reduce the total number of anchors and installations. Two different multiline geometries are studied—a 3-line anchor system and a 6-line anchor system. Simulations of the anchor forces are generated using National Renewable Energy Laboratory's OC4-DeepCwind semisubmersible floating system and 5-MW wind turbine, and the anchor forces of the 2 different multiline geometries are compared to those of a conventional single-line anchor geometry. Multiline anchor net force is calculated by vector summing the contributing tensions of the lines connected to the anchor. Results show that the behavior of the multiline anchor net force is governed by the connected line contributing the largest tension. Mean and maximum anchor forces are decreased in the 3-line anchor system and increased in the 6-line anchor system, relative to the single-line system. The average direction of multiline anchor net force is aligned with environmental load direction, and a wider range of multiline anchor net force directions are exhibited for wave-dominated load cases. Direction reversal of the multiline anchor net force under constant wind, wave, and current direction is small and infrequent. These force direction results reveal that a multiline anchor must have axisymmetric strength.

KEYWORDS

anchors, floating wind turbines, mooring, multidirectional loading, multiline, offshore wind energy

1 | INTRODUCTION

The offshore wind industry has shown a steady trend towards larger turbines being installed in deeper water in locations further offshore.[1] These new potential areas of offshore wind development in deeper water offer access to higher, more consistent wind resources and remove the concern of shoreline aesthetics. The depth limitations of fixed-bottom offshore wind turbines (approximately 60 m)[2] motivates the development of floating concepts. Therefore floating offshore wind turbines (FOWTs) hold great potential as the next step in the offshore wind energy industry.

A primary obstacle in floating offshore wind development is the high capital cost associated with constructing the large platforms and mooring systems needed to support the turbines in deep water.[3] The magnitude of the support structure cost relative to the total cost encourages research in support structure efficiency, which motivates the multiline anchor concept analyzed in this paper. In conventional concepts, each FOWT is moored separately by at least 3 single-line anchors. In the multiline concept (Figure 1), anchors are shared amongst FOWTs, allowing for a smaller

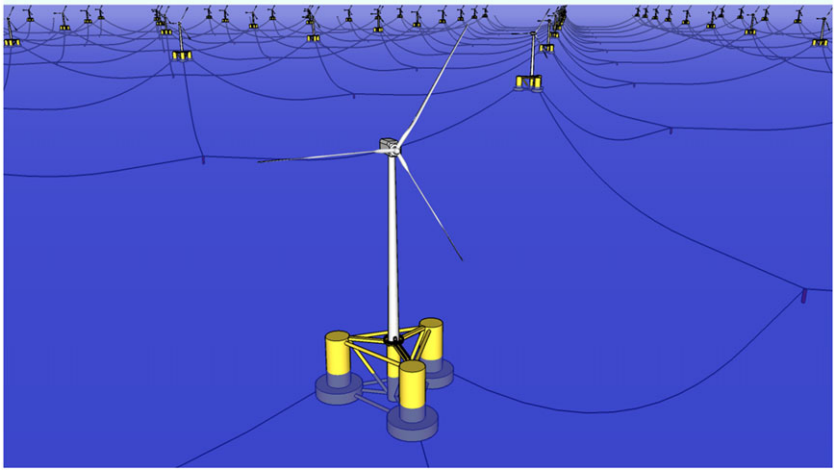

FIGURE 1 Floating offshore wind farm utilizing multiline anchor system [Colour figure can be viewed at wileyonlinelibrary.com]

number of anchors, site investigations, and installation operations. This paper explores this novel multiline anchor concept in terms of layout geometries and characteristics of the anchor forces.

2 | MULTILINE ANCHOR LAYOUT GEOMETRIES

The first step in evaluating the multiline anchor concept is generation of the multiline anchor geometries. Both the number of anchors per FOWT and the number of FOWTs per anchor can be modified to create new multiline geometries. The single-line system used for comparison in this research has 3 anchors per FOWT and 1 FOWT per anchor. The use of 3 mooring lines and anchors per FOWT is most common amongst FOWT demonstration projects (Hywind, WindFloat, and Hybrid Spar) and development concepts—almost half of the projects that disclosed mooring system information in the Carbon Trust's 2015 FOWT Review utilize 3-line mooring systems, compared with others using as little as 1 line to as many as 8 lines.[4] The multiline geometries in Figure 2 are developed with the following characteristics:

1. For simplicity in a potential wind farm, only multiline geometries that contain a repeating unit cell are used. In such a repeating unit cell geometry, the turbines connected to a multiline anchor are arranged concentrically around it, and the FOWT-FOWT, FOWT-anchor, and anchor-anchor spacing is consistent across a specific multiline geometry. As a result, the unit cells of a specific multiline anchor geometry can be easily multiplied to any farm size.
2. All systems evaluated—single-line anchor, 3-line anchor, and 6-line anchor—are nonredundant mooring systems because there are only 3 lines per FOWT.
3. The catenary mooring system design in terms of number of lines (3), radial distance from fairlead to anchor (797 m), each line length (835 m) and chain size (76 mm), is consistent across all systems evaluated (see Section 4.1, turbine, floating platform, and mooring system). The default 3-single-line system is patterned so that anchor locations become coincident, creating the multiline geometries (see Figure 2).

In terms of number of anchors, the most efficient geometry would be one that minimizes the ratio of anchors to turbines. More specifically, this would be a geometry that maximizes the number of FOWTs connected to each multiline anchor and minimizes the number of

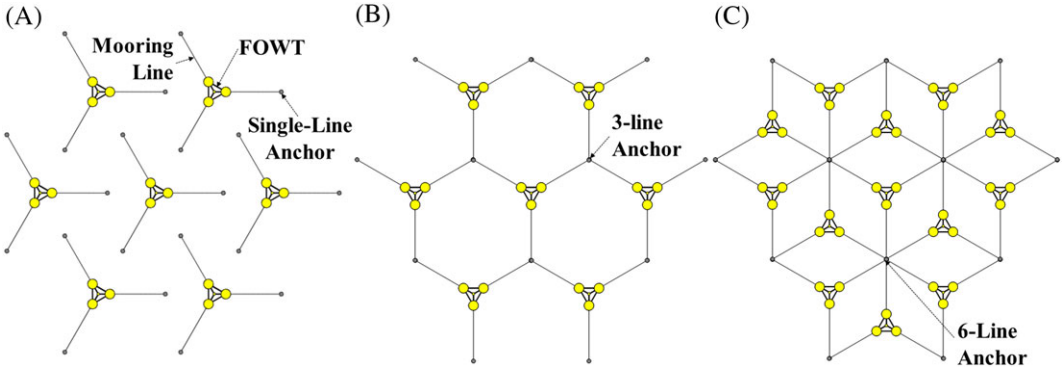

FIGURE 2 Layout of A, single-line; B, 3-line anchor; and C, 6-line anchor systems [Colour figure can be viewed at wileyonlinelibrary.com]

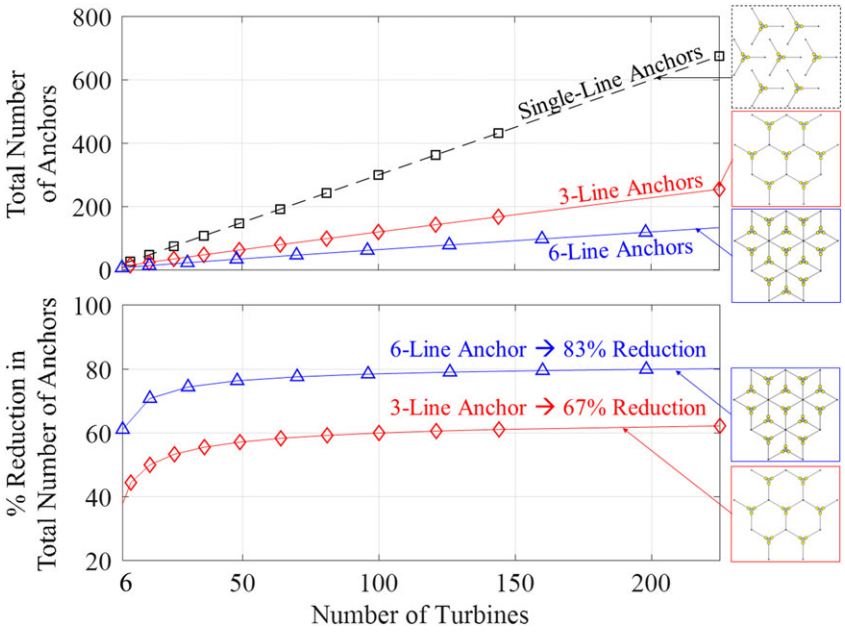

FIGURE 3 Total number of anchors for the single-line, 3-line, and 6-line geometries relative to farm size, and percent reduction in total number of anchors from single-line concept [Colour figure can be viewed at wileyonlinelibrary.com]

anchors used to moor each FOWT, subject to the constraint that an FOWT must be moored by at least 3 anchors ($n_{A/T} \geq 3$). Note that the number of anchors per turbine and number of turbines per anchor are not inverses of each other since, for example, a turbine may be moored by 3 anchors but each anchor may be connected to 6 turbines (see Figure 5). An approximation to the number of anchors required for a specified farm size is given by

$$N_A = N_T \times \frac{n_{A/T}}{n_{T/A}}, \tag{1}$$

where N_A is the total number of anchors required, N_T is the total number of FOWTs, $n_{A/T}$ is the number of anchors connected to each FOWT, and $n_{T/A}$ is the number of FOWTs connected to each anchor. The ratio of $n_{A/T}$ to $n_{T/A}$ can be thought of as a measure of the aforementioned efficiency in terms of number of anchors. This relationship neglects perimeter effects in which the anchors around the perimeter of the farm are connected to less FOWTs than the farm's overall $n_{T/A}$ value. The magnitude of this perimeter effect varies by multiline geometry and wind farm size. Perimeter effects become negligible for very large wind farms. Figure 3 presents the total number of anchors required relative to farm size for each geometry.

For a hypothetical commercial scale wind farm of 100 FOWTs, the use of 3-line or 6-line anchor systems would result in 60% or 79% reductions in total number of anchors required, respectively. The sharp increase in percent reduction at low numbers of FOWTs is result of sharply decreasing perimeter effects. This initial analysis is strictly limited to number of anchors and does not include cost of anchor materials or installation.

It is anticipated that floating wind installations may use larger capacity turbines than the 5-MW model used in this study.[1] While changes in turbine size has not been specifically studied in the context of the multiline anchor concept, it is possible that larger turbines may mean fewer turbines per farm, so the percent reduction in number of anchors and installations may be lower (note the scale effects in Figure 3).

3 | DEFINITION OF MULTILINE ANCHOR NET FORCE

A key goal of this work is to understand the dynamics of the multiline anchor net force, as this novel system in which a single anchor is loaded by multiple mooring lines from different directions has not been used for FOWTs in practice or explored in concept. This section is devoted to the description of the multiline anchor system and forces in order to clarify the following analysis of mean and fluctuating anchor forces, maximum anchor forces, and anchor force directionality.

In single-line anchor systems, the dynamics of the loading on the anchor is governed by a single line connected to it. In multiline systems in which anchors are shared amongst the FOWTs, the anchor is loaded by 3 or more lines simultaneously. This introduces the need to analyze the net multiline loading on the anchor and how it differs from the single-line loading.

In the following description of the multiline anchor system and forces, the subscript of a value identifies the connected FOWT. A visual representation of the FOWTs, lines, and multiline anchor for the 3-line anchor system is shown in Figure 4 where T_1, T_2, and T_3 are the line tensions from the connected FOWTs 1, 2, and 3 that make up the multiline anchor net force.

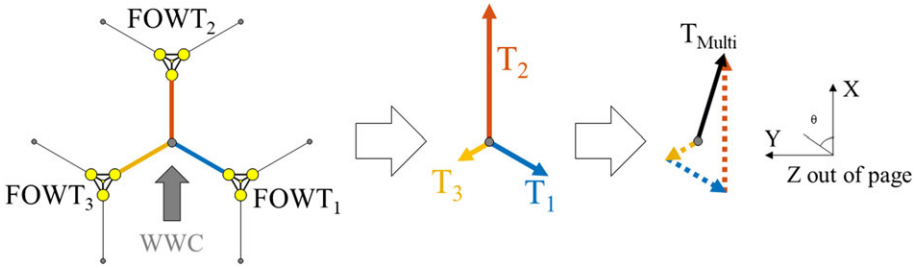

FIGURE 4 Diagram of multiline anchor net force from single-line contributing tensions of the 3 connected floating offshore wind turbines (FOWTs) for the 3-line anchor with 0° wind, wave, and current (WWC) direction. WWC direction is designated as θ, with 0° pointing to the top of the page, and 90° pointing to the left [Colour figure can be viewed at wileyonlinelibrary.com]

The multiline anchor net force is found with vector summation, given by

$$\boldsymbol{T}_{\boldsymbol{multi}}(t) = \sum_{i=1}^{n} \boldsymbol{T}_{\boldsymbol{i}}(t), \tag{2}$$

where $\boldsymbol{T}_{\boldsymbol{i}}$ is the vector containing the x, y, and z components of the contributing line tension at the shared anchor and n is the number of mooring lines connected to the anchor.

Since the mooring system is catenary, there is always a portion of line laying on the seabed, and there are no uplift forces on the anchor at the seabed. As a result, the z-component of any contributing single-line tension is always zero, and the magnitude of the multiline line anchor force in the XY plane, T_{multi}, can be simplified to

$$T_{multi}(t) = \sqrt{T_{multiX}(t)^2 + T_{multiY}(t)^2}, \tag{3}$$

where T_{multiX} is the sum of the X-components of the contributing line tensions and T_{multiY} is the sum of the Y components of the contributing line tensions. Furthermore, the direction of single-line anchor force in the XY plane has a range of less than 3° for the FOWT system of this study. This is a result of the very large fairlead-to-anchor distances (>800 m) relative to small platform motions (<20 m). Therefore, it can be reasonably approximated that the lines connected to the 3-line anchor apply tensions at 120° from one another (Figure 2B), and the lines connected to the 6-line anchor apply tensions at 60° from one another (Figure 2C). For the 3-line anchor,

$$T_{multiX}(t) = T_2(t) - \cos 60[T_1(t) + T_3(t)], \tag{4}$$

$$T_{multiY}(t) = \sin 60[T_3(t) - T_1(t)]. \tag{5}$$

And for the 6-line anchor,

$$T_{multiX}(t) = T_2(t) + \cos 60[T_4(t) + T_6(t) - T_1(t) - T_3(t)] - T_5(t), \tag{6}$$

$$T_{multiY}(t) = \sin 60[T_3(t) + T_4(t) - T_1(t) - T_6(t)], \tag{7}$$

where T_1, T_2, T_3, T_4, T_5, and T_6 are the magnitudes of the line tensions at the anchor from the connected FOWTs. This method of vector summations is supported by the work of co-author Landon's student, in which physical modeling of a suction caisson loaded orthogonally showed that the resultant load resistance of the multiline anchor correlated very well with the vector summation of the contributing line tensions.[5] This validation of the vector summation method for net multiline anchor force calculation is important in that multiple lines attached to a single anchor is a novel system; therefore, there are no specific standards that dictate how to calculate forces in this configuration.

4 | MODEL AND ANALYSIS METHODS

This section describes the FOWT model, simulation software, and environmental loading conditions used to generate time histories of the anchor force dynamics.

4.1 | Turbine, floating platform, and mooring system

The turbine chosen for this analysis is the National Renewable Energy Laboratory's (NREL) 5-MW reference turbine, and the support structure chosen is the OC4-DeepCwind semisubmersible floating system.[6] NREL's 5-MW reference turbine was developed to be representative of a typical utility-scale turbine and is widely used in the offshore wind energy research community.[7] The OC4-DeepCwind semisubmersible floating

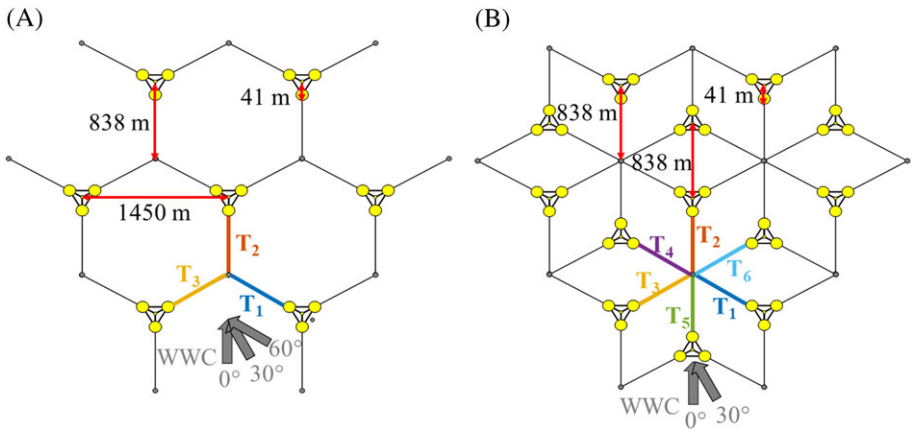

FIGURE 5 Spatial layout of the multiline anchor connection and OC4-DeepCwind floating system for A, 3-line anchors; B, 6-line anchors. Water depth = 200 m. WWC = wind, wave, and current [Colour figure can be viewed at wileyonlinelibrary.com]

TABLE 1 Properties of the OC4-DeepCwind semisubmersible floating system[8]

Mooring system	Catenary
Mooring line type	Studless chain
Extensional stiffness	753.6 MN/m
Water depth	200 m
Line length	835.35 m
Chain nominal diameter	0.0766 m
Mass per unit length chain	113.35 g/m

system was chosen because it employs the most commonly studied platform type (semisubmersible) and mooring system type (catenary) in current FOWT technology/concepts.[4] The buoyancy-stabilized semisubmersible platform also possesses a variety of advantages, including suitability in any water depth, low installation vessel requirements, onshore assembly, and towing stability.[4] Spatial layout of the OC4-DeepCwind floating system for 3-line and 6-line multiline anchor geometries are shown in Figure 5, and relevant properties of the OC4-DeepCwind mooring system are provided in Table 1.[8] The 3-line and 6-line anchor geometries result in interturbine spacings of 1451 and 838 m, respectively. The spacing of the 3-line system is consistent with the spacing of the first and only floating offshore wind farm—Hywind Pilot Park—which consists of 5 FOWTs and employs a spacing of 1386 m.[9] It should be noted, though, that the Hywind project is installed in water depths of 95–120 m,[9] which is shallower than the 200-m water depth of the OC4-DeepCwind floating system model.[6,8] The contributions of line tensions from FOWTs 1, 2, and 3 are the same for the 3-line and 6-line anchor system, and the 6-line anchor system has an additional 3 FOWTs connected to the anchor.

4.2 | Simulation software and mooring model

The dynamics of the FOWT system are modeled with NREL's FAST (Fatigue, Aerodynamics, Structures, and Turbulence) Code. FAST v8 is a comprehensive, fully coupled aero-hydro-servo-elastic simulator capable of predicting motions and loads in the time domain.[10,11] Mooring line and anchor force dynamics were simulated via MoorDyn, a lumped-mass mooring model within FAST. MoorDyn was chosen out of the 3 available mooring models in FAST for its combination of accurate prediction of mooring dynamics and high computational efficiency. The model accounts for mooring line axial stiffness and damping, weight and buoyancy forces, and hydrodynamic forces from Morison's equation.[12] Line properties for the OC4-DeepCwind mooring system in the MoorDyn input file are taken from Hall and Goupee.[13] Furthermore, MoorDyn has been validated against experimental test data and industry standard software to yield accurate results for mooring dynamics.[13]

The American Bureau of Shipping Guide for Building and Classing FOWTs requires friction force be included in the calculation of anchor force,[14] as friction between the mooring line and seabed can have a significant effect on anchor forces, especially in catenary mooring systems where large portions of the chain are resting on the seabed.[15] Friction force is not currently included in MoorDyn. FAST models the anchor as a fixed point at the seabed surface, but it should be noted that this simplification does not affect mooring line dynamics. For this paper, seabed friction was applied to the anchor force in a postprocessing routine. Time histories of the mooring line lay length were first determined from MoorDyn node location output, and seabed friction force, $F_{friction}$, was calculated by

$$F_{friction}(t) = fL(t)W_{sub}, \tag{8}$$

where t is the time, f is the coefficient of static friction between the chain and the seabed, taken here as 1.0 as given by American Bureau of Shipping,[14] L is the lay length of the mooring line on the seabed, and W_{sub} is the submerged unit weight of the mooring line.[14] Anchor forces from

TABLE 2 Details of environmental loading conditions[16]

Load Case	DLC 1.2	DLC 1.6	SLC
Conditions	Normal operating (fatigue)	Extreme operating (strength)	Extreme nonoperating (strength)
Wind speed at hub height	10.2 m/s	11.4 m/s (rated)	45 m/s (500-yr)
Turbulence intensity	9%	10%	10%
Significant wave height	2.7 m	8.0 m (50-yr)	12 m (500-yr)
Peak spectral wave period	7.0 s	12.7 s	15.3 s
JONSWAP gamma factor	2.5	2	2.5
Current speed	0.23 m/s	0.30 m/s	0.55 m/s

Abbreviations: DLC, design load case; SLC, survival load case.

FAST outputs then were subsequently decreased by the force of the seabed friction at each time step. The number of segments per line used for the lumped-mass mooring dynamics model was increased from 20 to 165 to increase the accuracy of the lay length time history. Friction forces may change slightly over time, but in this study, the ABS recommended approach described above has been used.

4.3 | Environmental conditions

It is important to evaluate the dynamics of the multiline anchor net force over a wide range of environmental and operating conditions. In an effort to narrow down the combination of WWC parameters to test, several critical design load cases (DLCs) are selected for this analysis, shown in Table 2. These cases include both operating and nonoperating, and both normal and extreme conditions. Most importantly, the governing environmental load is different for each case, which allows for differentiation of the multiline anchor load effects between each type of environmental loading. Governing load refers specifically to wind or waves, as current loads are typically much smaller. DLC 1.2 is wind dominated, DLC 1.6 is wind-and-wave dominated, and the survival load case (SLC) is wave dominated.

The WWC parameters for these 3 critical environmental conditions are taken from the full-scale VolturnUS project,[17] harvested from over 10 years of buoy data at a site off Monhegan Island, Maine.[18,19] The water depths of the OC4-DeepCwind FOWT and the full scale VolturnUS project are 200 and 168 m, respectively. Therefore, the environmental conditions were deemed to be suitable for use in this study. The wind speed in DLC 1.6 of 11.4 m/s is the rated wind speed of the NREL 5-MW reference turbine that produces peak thrust,[7] as designated in American Bureau of Shipping.[14] The turbulent wind field is generated with a Kaimal spectrum via Turbsim.[20] Waves are generated with a JONSWAP spectrum, and wave heights are Rayleigh distributed,[21] consistent with the modeling choices in Coulling et al.[6] Current is steady and equal at each FOWT. Co-directional WWC directions of 0°, 30°, and 60° are evaluated for the 3-line anchor geometry, and directions of 0° and 30° are evaluated for the 6-line anchor geometry. The range of 0° to 60° is suitable for capturing the range of important dynamics for the 3-line anchor system because the geometry has 120° rotational symmetry. For the 6-line case, only 0° to 30° WWC directions are needed because the 6-line anchor geometry has 60° rotational symmetry (see Figure 5). Furthermore, these direction ranges of WWC are also appropriate because yaw misalignment is not included. Six 1-hour simulations using different random seeds were completed for each combination of load case and WWC direction.

Each of the FOWTs connected to the multiline anchor are subjected to independent wind fields and independent wave fields; therefore, wind wake effects and spatial coherence of the waves are not included.[22] As a rule of thumb, wind wake effects can be neglected when the turbines are spaced more than 10 rotor diameters apart.[23] The NREL 5-MW reference turbine has a rotor diameter of 126 m, making the turbine spacing at which wake effects can be considered negligible 1260 m. In the 3-line anchor system, the turbine spacing is 1451 m, and the assumption of negligible wake effects is appropriate in this case. In the 6-line anchor system, the turbine spacing is 838 m, and wake effects are not negligible in this case. For example, the decrease in wind speed due to wake effects from 11.4 to 9 m/s[23] would decrease the rotor thrust from 800 kN to roughly 500 kN[24] in DLC 1.6 for the 6-line anchor system. Including wake effects in this stage significantly increases the number of permutations of conditions with WWC directions; therefore, they are not considered in this study. However, the inclusion of wake effects in a farm scale analysis of the multiline concept is an ongoing subject of research for the authors, as it is likely to produce some changes in the mooring line tensions and anchor forces.

Furthermore, the connected FOWTs are subjected to independent wave fields, and spatial coherence of the waves is not included. This decision is supported by previous work from the authors, which concluded that there was no significant difference between anchor force characteristics for connected turbines loaded by spatially coherent waves versus with independent waves.[22] Additional ongoing work on this topic has further shown that correlation in coherent wave fields is insignificant for points separated by more than several hundred meters, depending upon wave parameters.

5 | MULTILINE ANCHOR LOADING DYNAMICS

Using multiline anchors for FOWTs is a novel idea; therefore, it is important to examine a wide variety of dynamic effects on the anchor loading. This section will examine general trends, mean and maximum forces, and directionality of the multiline anchor net force.

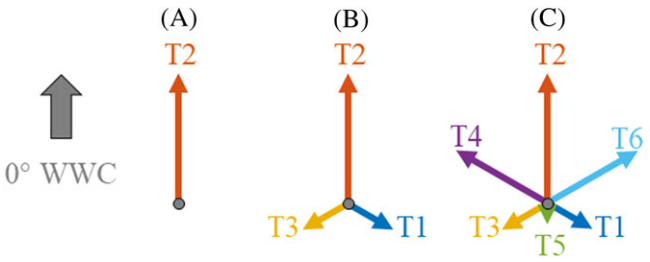

FIGURE 6 Line tension(s) contributing to anchor force for A, single-line anchor; B, 3-line anchor; and C, 6-line anchor. Line tension vectors are proportional to mean tensions in DLC 1.2 with 0° wind, wave, and current (WWC) direction [Colour figure can be viewed at wileyonlinelibrary.com]

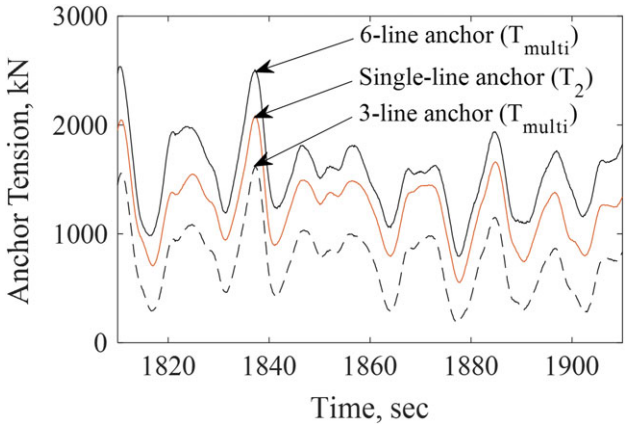

FIGURE 7 Comparison of same peak force event for single-line, 3-line, and 6-line anchor system [Colour figure can be viewed at wileyonlinelibrary.com]

5.1 | Anchor force magnitude and variation

Due to the direction of environmental loads chosen for this study, T_2 is greater than or equal to the largest contributing tension in all load cases and WWC directions because it is connected to the one of the FOWTs that is most directly downwind of the anchor (see Figure 5). Therefore, comparisons of forces will be made between the multiline anchor net force, T_{multi}, and T_2 from the single-line case. The multiline anchor net force in the 3-line anchor system is a combination of line tensions T_1, T_2, and T_3, (Equations (4) and (5)), and the multiline anchor net force in the 6-line anchor system is the same combination of T_1, T_2, and T_3, plus the additional contributions of T_4, T_5, and T_6 (Equations (6) and (7)), as shown in Figure 6.

The use of the same tensions between these different scenarios allows for a more direct comparison of the multiline anchor loading dynamics between single-line loading, 3-line anchor loading, and the 6-line anchor loading. An example of this direct comparison is shown in Figure 7, where a specific peak force event on the single-line anchor (T_2) is reduced under the loading of the 3-line anchor system and increased under the loading of the 6-line anchor system.

Examples of multiline anchor net force time histories, maximum forces, and contributing mean tensions are shown in Figure 8. While the magnitude of the specific contributing tensions in Figure 8 change with load case and direction, there are some general characteristics that should be noted. First, there is a significant range in the contributing tensions on the multiline anchor. Second, symmetry of the mooring system configuration and WWC directions results in many cases where some of the contributing line tensions are approximately equal (ie, T_1 and T_3 in the 3-line anchor, T_4 and T_6 in the 6-line anchor). Most importantly, the mean and maximum anchor force is decreased in the 3-line anchor system and increased in the 6-line anchor system, relative to the single-line system.

A broader evaluation of the single-line and multiline anchor net forces can be accomplished by comparing the mean, maximum, and standard deviation of the forces, as shown in Table 3. In general, the mean, maximum, and standard deviation are lower for the 3-line anchor and higher for the 6-line anchor, compared with the single-line anchor. This trend can be understood by revisiting the vector sum of the line tensions in each geometry and noting the direction of each line's tension components (see Figure 6). The maximum contributing single-line tension (T_2) is always applying force directly in the positive X direction (upwards on this page). In the 3-line anchor system, T_1 and T_3 always have components in the negative X direction (downwards on this page), opposite of the governing maximum contributing tension. Therefore, these contributing line tensions are only able to cancel out force in the X direction, never adding to it. In contrast, the 6-line anchor has additional contributing line tensions—T_4 and T_6—that have components in the same direction as the maximum contributing single-line tension T_2 (positive X); therefore, the

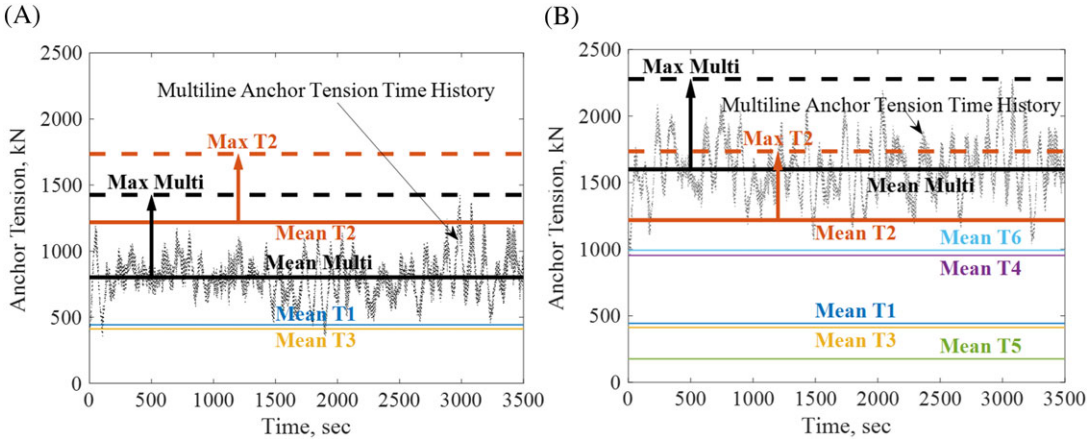

FIGURE 8 Time history of multiline anchor net force, means of contributing line tensions, and maxima of the maximum contributing single-line (T_2) and multiline anchor net forces in wind-dominated normal operational design load case 1.2 with 0° wind, wave, and current direction for A, 3-line anchor and B, 6-line anchor [Colour figure can be viewed at wileyonlinelibrary.com]

TABLE 3 Mean, maximum, and standard deviation of the single-line and multiline anchor net forces in kN[a] [Colour table can be viewed at wileyonlinelibrary.com]

		0° WWC Direction			30° WWC Direction			60° WWC Direction		
		Single-Line	3-Line	6-Line	Single-Line	3-Line	6-Line	Single-Line	3-Line	6-Line
Maximum, kN	DLC 1.2	1726	−19%	29%	1672	−22%	31%	1411	−16%	58%
	DLC 1.6	2560	−16%	20%	2250	−18%	32%	1610	−16%	90%
	SLC	3767	−11%	8%	3283	−13%	27%	2127	−14%	91%
Mean, kN	DLC 1.2	1218	−34%	32%	1165	−30%	38%	987	−18%	63%
	DLC 1.6	1238	−33%	34%	1194	−29%	40%	1019	−17%	63%
	SLC	1166	−32%	27%	1099	−27%	36%	923	−17%	60%
Standard Deviation, kN	DLC 1.2	116	19%	53%	114	4%	49%	119	−9%	49%
	DLC 1.6	280	0%	14%	229	−7%	28%	148	−12%	116%
	SLC	581	−14%	3%	476	−25%	20%	238	−16%	152%

Abbreviations: DLC, design load case; SLC, survival load case; WWC, wind, wave, and current.

[a]Red shading shows percent increase from single−line anchor value, and green shading shows percent decrease from single-line anchor value.

vector sum results in an addition of tensions, instead of a cancellation. It should be noted that the 0° and 60° WWC direction for the 6-line case are identical loading scenarios.

Section 2 revealed that the 3-line and 6-line anchor geometries can reduce the total number of anchors required for a floating offshore wind farm, but due to differences in loading, these anchors also must be designed with different strengths. The key loading for this comparison is the maximum anchor force, as this value governs anchor design. In this study, the analyses used to determine the maximum anchor force required for design are the critical strength load cases, DLC 1.6 and SLC. It should be noted that in a true design, a larger number of DLCs would need to be completed to determine the maximum anchor force. The design force is determined from whichever WWC direction produces the largest anchor force. In almost all cases, this is the 0° WWC. The only situation for which this does not hold true is the 6-line anchor system in the SLC case, where the 30° WWC direction results in a larger maximum force than the 0° WWC direction. The results of the maximum anchor force data reveal that a multiline anchor used in the 3-line anchor system would require less strength than its single-line counterpart, while a multiline anchor in the 6-line anchor system would require more strength.

It can also be observed that for a given multiline configuration (3-line or 6-line), the mean multiline anchor net force is nearly identical across all WWC directions for given a load case—less than 4% different. This is due to the way that the contributing line tensions change with respect to each other as the WWC direction changes—as some lines transition to lower tensions, others transition to higher tensions, resulting in very little change in the mean of the net multiline anchor net force. Although the mean force experiences little change, the direction of the multiline anchor net force changes significantly.

The behavior of the multiline anchor net force is governed by the line contributing the largest tension, which is T_2 in all load cases and WWC directions. This governing nature of the maximum contributing line is clearest for the cases where waves are the dominant environmental load (DLC 1.6 and SLC), as shown in the example in Figure 9.

This governing nature of T_2 is also relevant in the comparison of anchor forces for different WWC directions. For the 3-line anchor, the largest controlling nature of T_2 occurs in the 0° WWC direction. In the 30° and 60° WWC direction, the governing line tension T_2 is decreased, and the

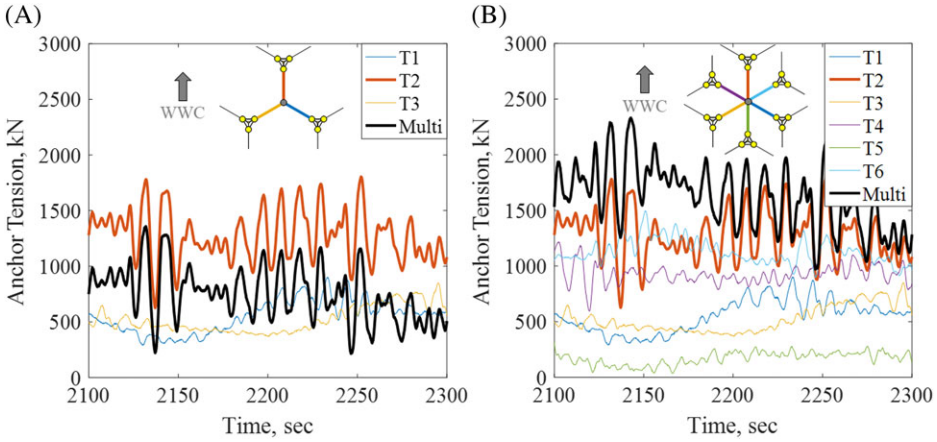

FIGURE 9 Contributing line tensions and multiline anchor time history in wind-and-wave dominated extreme operational design load case 1.6 with 0° wind, wave, and current (WWC) direction for A, 3-line anchor and B, 6-line anchor, showing governing behavior of the high T_2 [Colour figure can be viewed at wileyonlinelibrary.com]

new governing contributing line tensions (T_2 and T_3) are closer in magnitude. These more balanced contributing line tensions reduce the multiline anchor net force cycle amplitudes as shown in Figure 10. This is because there is a greater proportion of the force being cancelled, as the components of large controlling T_2 and T_3 tensions in the direction perpendicular to the WWC direction are more equal but opposite. This trend is not present in the 6-line anchor system due to larger number of contributing line tensions. In the 0° WWC direction for the 3-line system, the multiline anchor behaves very much like the single-line anchor because the contributions from the other lines (T_1 and T_3) are very small. In contrast, the

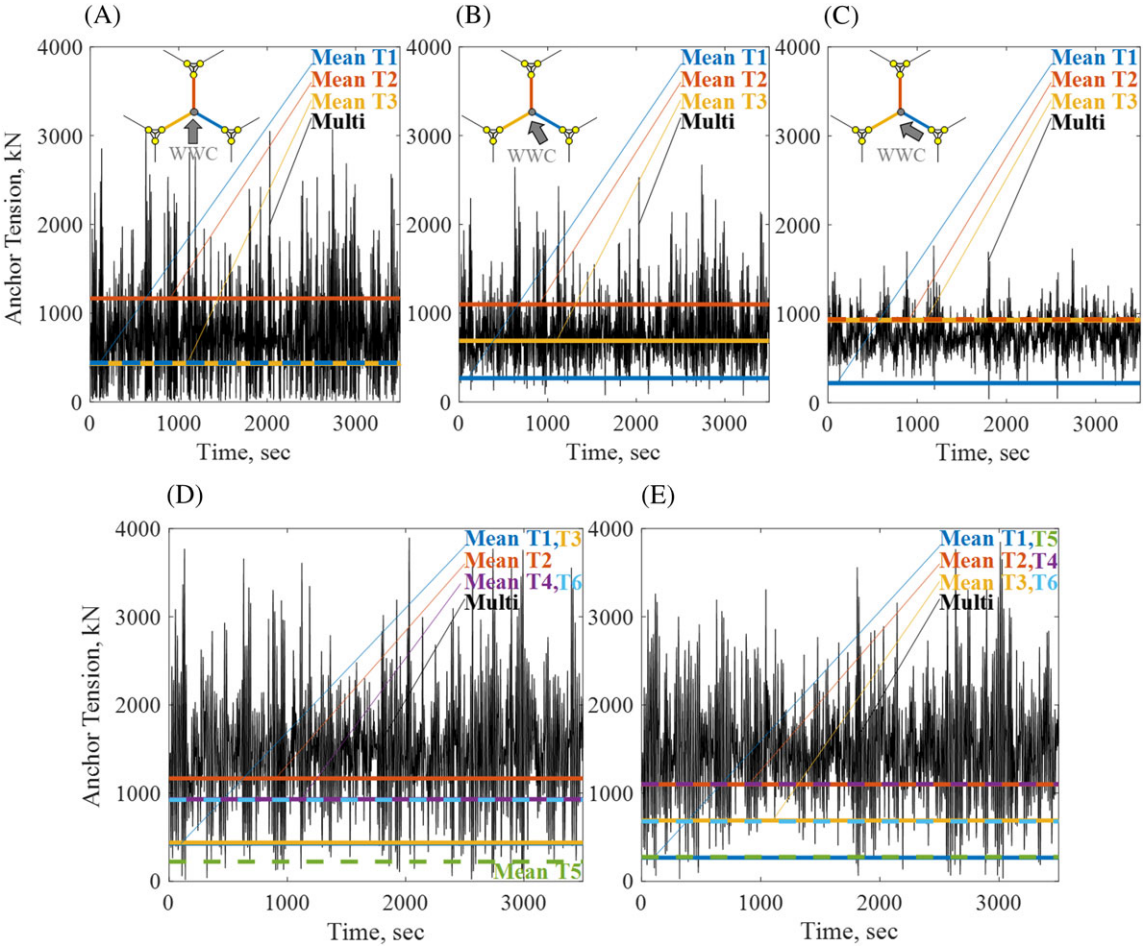

FIGURE 10 Multiline anchor time histories and mean contributing tensions in wave-dominated survival load case for the 3-line anchor for A, 0° wind, wave, and current (WWC); B, 30° WWC, and C, 60° WWC direction, and in the 6-line anchor for D, 0° WWC and E, 30° WWC [Colour figure can be viewed at wileyonlinelibrary.com]

6-line system always has more than one line contributing a significant portion of the net force, and therefore consistently has more balance between the governing tensions.

5.2 | Directionality

A primary difference between the single-line anchor force and the multiline anchor net force is the directionality, and this directionality must be assessed over a range of time scales: short (single force cycle), medium (1-h time history with consistent WWC direction), and long (days to years with changing WWC direction). It is important to note that multidirectional lateral loading on offshore anchors is a novel concept; therefore, applicable anchor design standards do not provide guidance or commentary relative to this type of loading. However, small-scale physical modeling of a suction caisson loaded in multiple directions has been conducted, revealing multiline anchor peak resistance greater than that of a caisson loaded in a single direction.[25]

5.2.1 | Directionality over 1 hour

The forces on a single-line anchor come from one direction that has a range of less than 3° in this FOWT system, while the multiline anchor can be subjected to loading from any direction, depending on which contributing line tensions are largest (see Figure 4). Two characteristics of multiline anchor net force directionality in the 1-hour time scale are average direction and directional variation, which are given in Table 4. The maximum contributing single-line tension, T_2, always has an angle mean of 0° and standard deviation of less than 1°. This approximately 0° standard deviation of the direction of the single-line force is a result of mooring geometry—the radial distance from the fairlead to the anchor is 800 m, and the platform displacements that move the mooring line are less than 20 m; therefore, the single mooring line's orientation with the anchor remains nearly unchanged.

Results in Table 4 reveal that the average direction of the multiline anchor net force is aligned with the WWC direction. This can also be seen in the force direction rosettes for the 6-line anchor in Figure 11 and the 3-line anchor in Figure 12. While only several examples of force direction rosettes are given, the alignment of the multiline anchor net force direction with the WWC direction appears in all load cases and WWC directions for both multiline geometries. The percentage labels on the circular axes depict frequency of the direction.

These results can be understood by considering the flow of forces; all connected FOWTs have a force applied to them in the direction of the WWC, and the fixed-point anchors are the nodes resisting this force. Therefore, the collective force applied to all connected FOWTs is applied to the multiline anchor in the same direction. In almost all cases, the average direction of the multiline anchor net force is within 4° of the WWC direction. The only exception to this is the 3-line anchor in SLC with 30° WWC, where the average direction is 10° different from the WWC

TABLE 4 Mean and standard deviation of multiline anchor net force angle

		0° WWC		30° WWC		60° WWC
		3-line	6-line	3-line	6-line	3-line
Angle Mean	DLC 1.2	−2°	−2°	28°	28°	58°
	DLC 1.6	−5°	−4°	28°	26°	57°
	SLC	3°	1°	40°	30°	60°
Angle Standard Deviation	DLC 1.2	10°	7°	11°	7°	10°
	DLC 1.6	17°	8°	14°	9°	12°
	SLC	53°	18°	32°	22°	23°

Abbreviations: DLC, design load case; SLC, survival load case; WWC, wind, wave, and current.

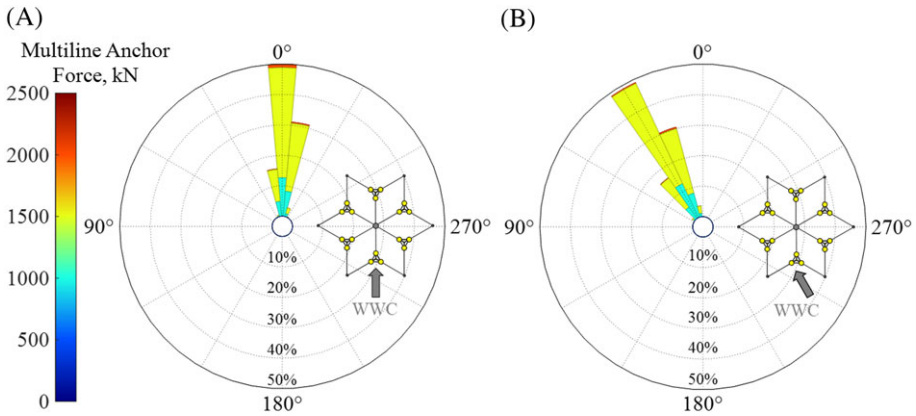

FIGURE 11 Direction rosettes for multiline anchor net force, example shown for 6-line anchor under wind-dominated design load case 1.2 loading with A, 0° wind, wave, and current (WWC) and B, 30° WWC [Colour figure can be viewed at wileyonlinelibrary.com]

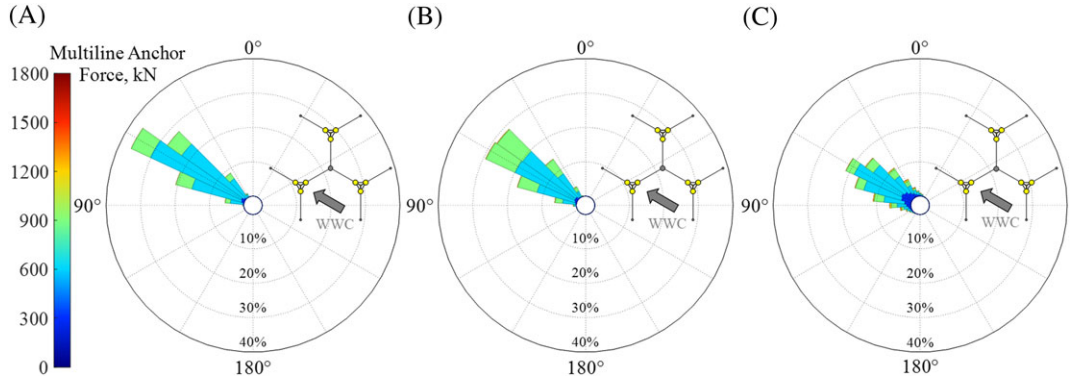

FIGURE 12 Direction rosettes for multiline anchor net force, example shown for 3-line anchor with 60° wind, wave, and current (WWC) under A, DLC 1.2 loading (wind dominated); B, DLC 1.6 loading (wind and wave dominated); and C, SLC loading (wave dominated) [Colour figure can be viewed at wileyonlinelibrary.com]

TABLE 5 Correlation coefficient between anchor force and wave elevation

	Single-line (Line 2 max Contributing)			3-line Anchor			6-line Anchor	
	0°	30°	60°	0°	30°	60°	0°	30°
DLC 1.2	0.09	0.11	0.10	0.07	0.09	0.06	0.06	0.06
DLC 1.6	0.72	0.70	0.44	0.68	0.64	0.28	0.62	0.45
SLC	0.84	0.85	0.83	0.77	0.75	0.39	0.79	0.56

Abbreviations: DLC, design load case; SLC, survival load case.

direction. This difference results from the specific combination of multiline geometry and load case. In the SLC, the waves are the dominant load (see Section 4.3), and they act primarily on the floating platform. In the 0° and 60° cases, the waves are hitting the platform along one of its lines of symmetry, but this is not the case for the 30° WWC direction. This wave loading along a line of asymmetry in the 30° case results in an asymmetry in the line tensions that is effectively translated to the anchor. The effect is not present in DLC 1.2 and DLC 1.6 because the wind load on the more symmetric rotor accounts for a larger portion of the loading, and the wind loading overshadows this effect of asymmetry in platform wave loading. Furthermore, this effect is also not present in the 6-line anchor system because although the asymmetry of the WWC direction and platform is still present, it is cancelled out by the symmetry of the 2 connected platforms loaded in this way (FOWTs 2 and 4, see Figure 5). The slight bias in average direction away from the WWC direction in the operational cases (DLC 1.2 and DLC 1.6) is a result of the small wind/rotor bias.

The results in Table 4 also show that the standard deviation of the multiline anchor net force direction increases as the load cases transition from wind dominated (DLC 1.2), to wind and wave dominated (DLC 1.6), to wave dominated (SLC). While this behavior is true of all load cases and WWC directions for both multiline geometries, it is shown most clearly for the 3-line anchor with 60° WWC direction, as seen in the rosettes in Figure 12.

The difference between wind loading and wave loading on an FOWT must first be discussed to understand this behavior. Wind loading acts on the rotor and contributes primarily to mean platform position and anchor force. Wave loading acts on the platform and contributes primarily to the force cycles and maximum force. In other words, the turbulence of the wind is insignificant compared with the fluctuation of wave elevation, relative to anchor forces. Due to this characteristic of the wave loading, the contributing line tensions have much larger fluctuations in cases that are wave dominated, and this larger variation in contributing line tensions results in the wider range in multiline anchor net force and direction. This is further supported by a comparison of correlation coefficients between anchor force and wave elevation at $FOWT_2$ across the load cases, as shown in Table 5.

It is important to think about these directional results over the 1-hour time scale from a potential anchor design standpoint, for which there is one very important outcome. A wind farm may see WWC coming from any direction over the course of its 20- to 25-year lifetime, and since the multiline anchor net force is closely aligned with the WWC direction, a multiline anchor may see loading from any direction over the course of its operation. As a result, a multiline anchor must have axisymmetric strength. This is a valuable conclusion, in that catenary mooring line systems like the one in this FOWT typically use drag anchors, which do not have omnidirectional capacity. Therefore, different, but existing, anchor types must be investigated for the multiline application.[26]

5.2.2 | Directionality over a single load cycle

It has been shown that a multiline anchor can experience loading from any direction over the course of its design life and that the force direction is closely aligned with the WWC direction. It is also important to examine the variation in direction over a short time scale (on the order of a single force cycle), which can be from 7 to 15 seconds from wave loading.

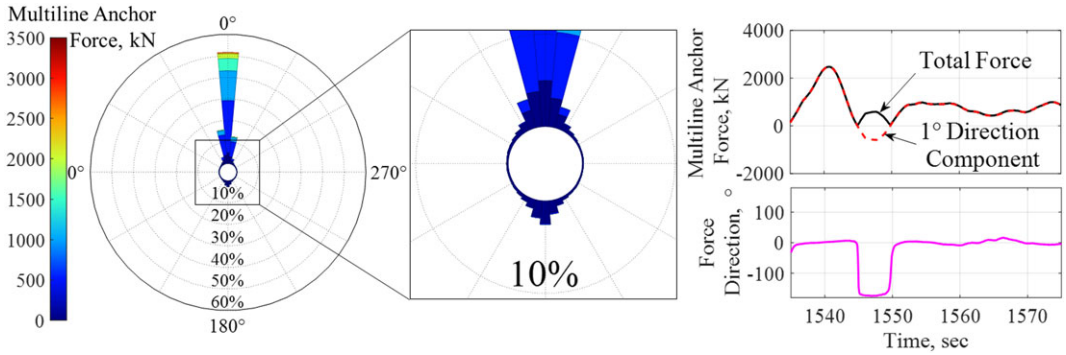

FIGURE 13 Direction reversal on 3-line anchor present in wave-dominated survival load case with 0° wind, wave, and current direction and 1° mean angle direction [Colour figure can be viewed at wileyonlinelibrary.com]

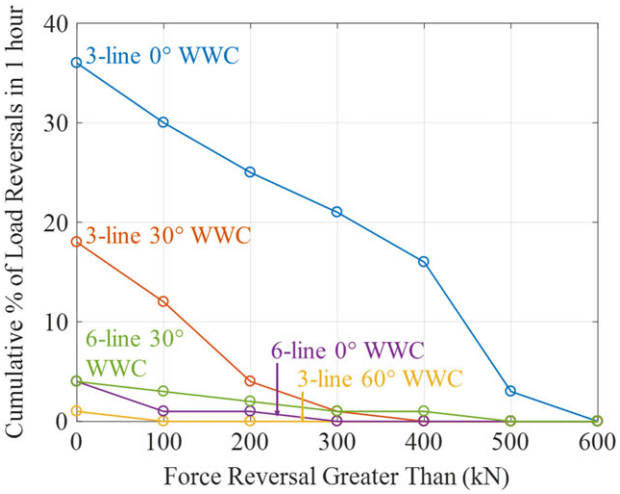

FIGURE 14 Cumulative percent of direction reversals relative to number of local minima in the component of the multiline anchor net force in the direction of the mean angle, for wave-dominated survival load case. WWC = wind, wave, and current [Colour figure can be viewed at wileyonlinelibrary.com]

In this paper, direction reversal refers to events in which the component of the multiline anchor net force in the mean angle direction (Table 4) reverses to the opposite direction, as shown in the rose plot and time history of Figure 13. The cumulative percent of direction reversals in SLC are shown in Figure 14. Percent direction reversals are calculated relative to the number of local minima in the time history of the component of the multiline anchor net force in the direction of the mean angle, and these percentages are averaged across 6 seeds.

Direction reversal of the multiline anchor net force occurs most in this study under the 3-line anchor geometry in the SLC with 0° WWC direction. The higher occurrence of direction reversal in SLC is due to a combination of the large waves and small mean platform offset, which means that the governing contributing tension is experiencing higher amplitude cycles at a lower mean force. Direction reversal is not a result of the nongoverning lines contributing higher tensions, but rather the governing line dipping to a very low tension. This commonly occurs following a peak tension event, after which the governing line (T_2) drops low enough that the other lines (T_1 and T_3) temporarily become the largest contributing tensions. Since the collective contribution of T_1 and T_3 is in the opposite direction of the normally governing T_2, direction reversal occurs.

While direction reversal is thought to be detrimental to offshore foundation performance,[27] there are several characteristics that reduce this concern, the first of which is the infrequent nature of this behavior. Direction reversal does not occur at all in the normal operating load case (DLC 1.2), which approximates the most likely conditions the FOWT is to experience for the majority of its design life. Direction reversal occurs rarely in the extreme operating case (DLC 1.6)—only for the 3-line anchor with 0° WWC direction, and in this situation, less than 3% of the time. While direction reversal does happen frequently in the SLC, the SLC has a small probability of occurring in the FOWT's design life, and therefore, the probability of the direction reversal has a small likelihood as well. SLC is important for the determination of peak force events for use in anchor design strength but is not as relevant for cyclic analysis. Since direction reversal is a cyclic loading concern, it is only anticipated to be a significant design consideration if it occurs frequently in a more probable DLC, namely, those used in fatigue analysis. It should be noted that the critical design load case DLC 6.1, with nonoperational 50-year storm conditions, is not included in this analysis and is also expected to have occurrences of direction reversal.

TABLE 6 Maximum multiline anchor net force in direction of the mean angle (compare with small force reversal magnitudes in Figure 14) and mean force reversal as a percent of the peak force that occurs just before reversal

	3-line Anchor			6-line Anchor	
WWC direction	0°	30°	60°	0°	30°
Maximum force in direction of mean angle, kN	3347	2650	1487	4047	4055
Mean of force reversal as percent of previously occurring peak force, %	17	10	6	4	8

Abbreviations: DLC, design load case; SLC, survival load case; WWC, wind, wave, and current.

In addition, while the multiline anchor net force does reverse direction, the magnitudes of the force direction reversals in Figure 14 are relatively small compared to the maximum multiline anchor net force in the direction of the mean angle as shown in the Table 6. Table 6 also shows the mean value of the force reversal as a percent of the previously occurring peak force in the opposite direction.

When a direction reversal occurs in a force cycle, the mean of the force cycle is still heavily nonzero. This is an important distinction to make for an offshore anchor, as mean zero force cycles can lead to capacity reduction, while offset mean can lead to capacity increase.[27] Even in the most extreme realization of direction reversal, the reversed force is only 33% of the previous peak force in the mean direction, and the mean of the cycle is highly nonzero at 730 kN. However, the nature of multiline anchor net force direction range and reversal may be affected by extreme weather events with extreme wind directional changes, and this impact is an ongoing topic of study for the authors.

6 | CONCLUSIONS

A multiline anchor concept is evaluated in which FOWTs share anchors, in an effort to lower FOWT support structure costs. Results of this analysis are compared to conventional single-line anchor loading. It is shown that the implementation of the multiline anchor system in a floating offshore wind farm would result in large reductions in the total number of anchors required—60% in the 3-line anchor system and 79% in the 6-line anchor system for a typical commercial scale 100-turbine floating offshore wind farm. The average maximum anchor force differs significantly for the multiline anchor compared with the single-line anchor, decreasing by 16% in the 3-line anchor and increasing by 20% in the 6-line anchor for DLC 1.6, and decreasing by 11% in the 3-line anchor and increasing by 10% in the 6-line anchor for the SLC. Therefore, the design strength of the multiline anchor would be different than its single-line counterpart.

It is also shown that a multiline anchor will be subjected to loading from any direction over the course of its design life, as the average direction of multiline anchor net force is aligned with the direction of the environmental load. Furthermore, force direction reversals within a single force cycle are present in extreme cases for the multiline anchor. A variety of anchor types with axisymmetric strength exist that can perform appropriately under such multidirectional loading conditions and differ from drag anchors that are being considered for mooring of single-line FOWTs. Suitability of different anchors for the multiline concept is discussed in Diaz et al.[26] Other important considerations not examined in this paper include effects of anchor placement accuracy and increased number of padeyes per anchor.

Future work includes studying the multiline anchor concept on a large commercial farm scale. The turbine interconnectedness produced by the multiline anchor concept necessitates the evaluation of spatial wave coherence and wake modeling throughout the farm, relative to multiline anchor net force behavior. A preliminary investigation of spatial wave coherence is provided in the author's previous work,[22] and further examination has revealed that there is no significant relationship between wave fields at turbines connected to the multiline anchor for typical offshore wind turbine spacing.

The anchor force results in Section 5 are specific to the OC4-DeepCwind semisubmersible floating system. However, general conclusions about multiline anchor systems with catenary mooring systems can still be made from this work, namely, that multiline anchor forces will be significantly different from single-line anchor forces, mean direction of force will be aligned with the WWC direction, and force directional reversal may be present. Furthermore, due to the sensitivity of mooring line and anchor dynamics to mooring configuration, exploration into multiline anchor net force behavior with changes to spatial parameters, namely, turbine spacing and water depth, is an ongoing topic of investigation by the author.

ACKNOWLEDGEMENTS

This work is generously funded by US National Science Foundation grants IGERT-1068864, CMMI-1463273, CMMI-1463431, and CMMI-1462600 and the Massachusetts Clean Energy Center.

ORCID

Casey M. Fontana http://orcid.org/0000-0002-6843-7722

REFERENCES

1. U.S. Department of Energy. Offshore wind technologies market report; 2016.

2. U.S. Department of Energy. National offshore wind strategy.; 2016.
3. International Renewable Energy Agency. Floating foundations: a game changer for offshore wind power.; 2016.
4. Carbon Trust. Floating offshore wind: Market and technology review.; 2015.
5. Chung J. Physical modeling of suction caissons loaded in two orthogonal directions for efficient mooring of offshore wind platforms. 2012. https://digitalcommons.library.umaine.edu/etd/1754
6. Coulling AJ, Goupee AJ, Robertson AN, Jonkman JM, Dagher HJ. Validation of a FAST semi-submersible floating wind turbine numerical model with DeepCwind test data. *J Renew Sustain Energy*. 2013;5(2). https://doi.org/10.1063/1.4796197
7. Jonkman JM, Butterfield S, Musial W, Scott G. Definition of a 5-MW reference wind turbine for offshore system. *Development*. 2009. https://doi.org/10.1002/ajmg.10175
8. Robertson A, Jonkman J, Masciola M, et al. Definition of the semisubmersible floating system for phase II of OC4.; 2014. https://www.nrel.gov/docs/fy14osti/60601.pdf
9. Statoil. Hywind Scotland pilot park environmental statement.; 2015.
10. Jonkman B, Jonkman J. FAST v8.16.00a-Bjj.; 2016. https://wind. nrel.gov/nwtc/docs/README_FAST8.pdf
11. Jonkman JM, *Buhl Jr*. ML. *FAST User's Guide*.; 2005. https://doi.org/10.2172/15020796.
12. Hall M. MoorDyn user's guide.; 2017. http://www.matt-hall.ca/files/MoorDyn-Users-Guide-2017-08-16.pdf
13. Hall M, Goupee A. Validation of a lumped-mass mooring line model with DeepCwind semisubmersible model test data. *Ocean Eng*. 2015;104:590-603. https://doi.org/10.1016/j.oceaneng.2015.05.035
14. American Bureau of Shipping. Guide for building and classing floating offshore wind turbine installations.; 2014.
15. Thomas DO, Hearn GE. Deepwater mooring line dynamics with emphasis on seabed interference effects. In: Offshore Technology Conference; 1994. https://doi.org/10.4043/7488-MS
16. Viselli AM, Goupee AJ, Dagher HJ. Model test of a 1:8 scale floating wind turbine offshore in the Gulf of Maine. *J Offshore Mech Arct Eng*. 2015;137(4):041901. https://doi.org/10.1115/1.4030381
17. Viselli AM, Goupee AJ, Dagher HJ, Allen CK. Design and model confirmation of the intermediate scale VolturnUS floating wind turbine subjected to its extreme design conditions offshore Maine. *Wind Energy*. September 2015;2016(19):1161-1177. https://doi.org/10.1002/we
18. Pettigrew NR, Xue H, Irish JD, et al. The Gulf of Maine Ocean Observing System: generic lessons learned in the first seven years of operation (2001-2008). *Mar Technol Soc J*. 2008;42(3):91-102. https://doi.org/10.4031/002533208786842444
19. University of Maine. Mooring E0130: Central Maine Shelf, Gulf of Maine Moored Buoy Program, Physical Oceanography Group, School of Marine Sciences. http://gyre.umeoce.maine.edu/buoyhome.php. Published 2013.
20. Jonkman BJ, Kilcher L. TurbSim user's guide: version 1.06.00. *Natl Renew Energy Lab*. 2012. papers2://publication/uuid/0CDF5717-D4F8-4B8F-ABE8-A0C02844D1DE
21. Jonkman JM, Robertson AN, Hayman GJ. HydroDyn user's guide and theory manual.; 2015.
22. Fontana CM, Arwade SR, Hallowell ST, et al. Spatial Wave Coherence in Multiline Anchor Systems for Floating Offshore Wind Turbines. In: *International Conference on Structural Safety & Reliability*; 2017.
23. Renkema DJ. Validation of Wind Turbine Wake Models. 2007;32(5):459-475. https://doi.org/10.1260/030952408786411912
24. Xu BF, Wang TG, Yuan Y, Cao JF. Unsteady aerodynamic analysis for offshore floating wind turbines under different wind conditions. 2015; February;373(2035). https://doi.org/10.1098/rsta.2014.0080
25. Burns M, Maynard ML, Davids WG. Centrifuge modelling of suction caissons under orthogonal double line loading. *Int Conf Phys Model Geotech*. 2014;465-471. https://doi.org/10.1201/b16200-63
26. Diaz BD, Rasulo M, Aubeny CP, et al. Multiline Anchors for Floating Offshore Wind Towers. In: *Oceans*; 2016. https://doi.org/10.1109/OCEANS.2016.7761374
27. Andersen KH. Cyclic soil Parameters for Offshore Foundation Design. In: *International Symposium on Frontiers in Offshore Geotechnics*; 2015. https://doi.org/10.1201/b18442-4

How to cite this article: Fontana CM, Hallowell ST, Arwade SR, et al. Multiline anchor force dynamics in floating offshore wind turbines. *Wind Energy*. 2018;21:1177–1190. https://doi.org/10.1002/we.2222